Rotation function development of four-core fiber optic tweezers

Shang Gao (高 上) and Libo Yuan (苑立波)*

Key Laboratory of In-Fiber Integrated Optics, Ministry of Education, College of Science, Harbin Engineering University, Harbin 150001, China

**Corresponding author: lbyuan@vip.sina.com*

Received January 14, 2014; accepted March 15, 2014; posted online October 17, 2014

We demonstrate a new four-core fiber optic tweezers by polishing the end face of a four-core fiber into a truncated pyramid that is asymmetric to fiber cores. Optical intensity propagation and distribution are modeled numerically, and rotation function is developed by means of calculating three-dimensional trapping force and torque in ray optics regime. Simulation results show our tweezers is a feasible approach that can trap and rotate microscopic spheroid objects stably.

OCIS codes: 350.4855, 060.2310.
doi: 10.3788/COL201412.S20601.

Optical tweezers have found many important applications in biological and physical fields since Ashkin *et al.* first demonstrated a single-beam optical gradient force trap in 1986[1]. Later, the ability to rotate or spin microscopic particles greatly enhances the optical manipulation[2–4]. Standard optical tweezers using high numerical aperture objective lens are usually bulky and expensive, and low-cost and convenient fiber optic tweezers that can not only trap but also rotate microscopic objects have garnered significant attention. However, those fiber tweezers either are inconvenient because of two manipulation arms[5,6] or may produce unstable rotation[7]. Here we design a new micro-machined four-core fiber optic tweezers, give a simulation model in ray optics regime, and develop the rotation function by calculating three-dimensional optical intensity distribution and trapping torque of a spheroid particle.

The basic working principle is shown in Fig. 1. The four-core fiber end is polished into a truncated pyramid. The four slope faces form an angle θ with fiber's cross-section as shown in Fig. 1(b). Moreover, they are not symmetric about the fiber cores but rotate the same small angle δ (we name it rotation angle; black lines in Fig. 1(b)). Thus, the beams after deflection will not completely converge, and form into an optical vortex trap as shown by red arrows in Fig. 1. For sake of simplicity, we denote laser wavelength as $\lambda = 0.98$ μm, mode diameter $d_m = 8$ μm, core offset to fiber axis $d = 36$ μm, polished angle θ, rotation angle δ. We discuss forces and torques exerted on a dielectric spheroid particle with three axes $a = 3.5$ μm, $b = 1.5$ μm, $c = 3.5$ μm (c-axis along Z direction) and refractive index $n_s = 1.4$ in the optical vortex trap. Thus, we may use ray optics model in our simulation[8]. Our coordinate system is referenced as Fig. 1(b).

Beams out of fiber cores can be treated as Gaussian beam with a beam waist slightly less than 0.5 d_m due to refraction[9]. Let n_f and n_m be the refractive indices of the fiber and surrounding medium, respectively. Taking $n_f = 1.45$ and $n_m = 1.33$, and by using Snell's law we know the polished angle should be greater than the critical angle θ_c for total internal reflection, that is, $\theta > \theta_c = 66.5°$, so we take $\theta = 67°$. We name the points on Z-axis that are closest to beam axis "pseudo focus", which produces the maximum optical intensity along the Z-axis. Rotation angle has little influence on the "pseudo focus" position. Specifically, "pseudo focus" are around $z = 22.5$ μm (22.7, 22.6, 22.5, and 22.4 μm corresponding to 2°, 4°, 6°, and 8° rotation angle, respectively) The total optical intensity distribution is simply the superposition of four Gaussian beams neglecting the interference since the particle size is much greater than laser wavelength. Figure 2 clearly shows that generally the size of the optical vortex trap becomes larger as the rotation angle increases.

To calculate the optical force and torque in ray optics regime, we decompose the total light beam into individual rays, each with appropriate intensity and direction, and we neglect the influence of polarization state.

Consider first the force and torque due to a single ray of power P hitting a dielectric sphere as shown in

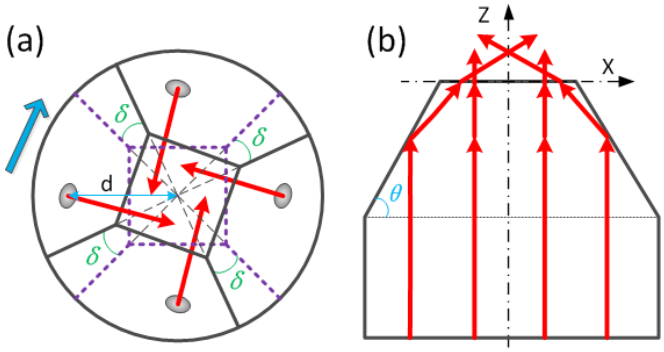

Fig. 1. Micro-machined triple core fiber end profile: (a) top view and (b) side view (blue arrow view direction in (a)).

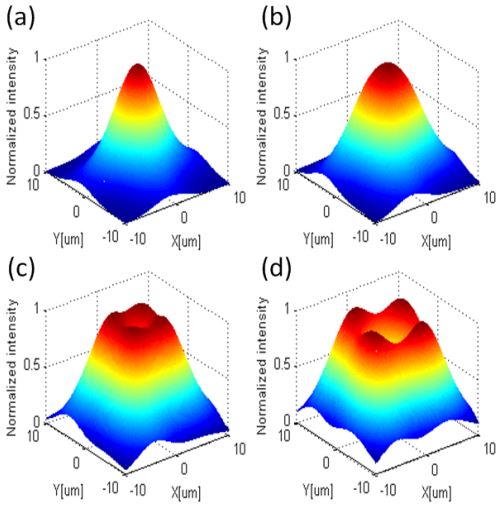

Fig. 2. Optical intensity distribution of z = "pseudo focus" plane with 67° polished angle when rotation angles are (a) 2° (b) 4°, (c) 6°, and (d) 8°, respectively.

Fig. 3. Denote the ray's total linear momentum per second as $\vec{p}$ and its magnitude is

$$\left|\vec{p}\right| = n_{\mathrm{m}} P/c, \tag{1}$$

where n_{m} is the medium refractive index and c is the light speed in vacuum. The force and torque exerted on the sphere particle due to the ith time reflection and transmission are

$$\vec{f}_{iR} = \vec{p}_i R - \vec{p}_{iR}, \vec{\tau}_{iR} = \vec{l}_{iR} \times \vec{f}_{iR}, \tag{2}$$

$$\vec{f}_{iT} = \vec{p}_i T - \vec{p}_{iT}, \vec{\tau}_{iT} = \vec{l}_{iT} \times \vec{f}_{iT}, \tag{3}$$

where R and T are the Fresnel reflection and transmission coefficients which depend on the incident angle, and $\vec{p}_i$, $\vec{p}_{iR}$, and $\vec{p}_{iT}$ are the momentums of the ith incident, reflected, and transmitted rays, respectively, and $\vec{l}_{iR}$ and $\vec{l}_{iT}$ are the corresponding lever arm pointing outward from the sphere center. Note that reflection never produces torques, that is, $\vec{\tau}_{iR} \equiv 0$. The total force and torque exerted on the sphere are sum of all the forces and torques that occur every time the ray reflects or refracts, namely

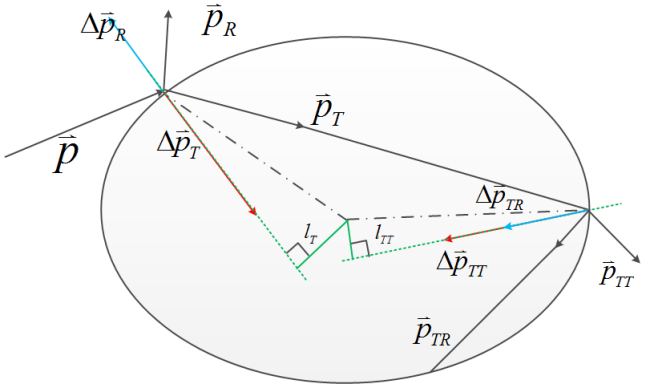

Fig. 3. Calculation method of forces and torques when a single ray hit on a particle.

$$\vec{f}_{\mathrm{total}} = \sum_{i=1}^{\infty} \vec{f}_{iR} + \vec{f}_{iT}, \tag{4}$$

$$\vec{\tau}_{\mathrm{total}} = \sum_{i=1}^{\infty} \vec{\tau}_{iT}. \tag{5}$$

Noting that the power of the ray decreases rapidly after each reflection and transmission, we can take the first few parts of Eqs. (4) and (5) as a quite accurate approximation.

From Eq. (1), it is easy to see that trapping force and torque are linearly proportional to laser power. Therefore, we mainly focus on the influence of rotation angle δ with our initial conditions as before setting total laser power to be 80 mW uniformly distributed in each fiber core.

Working point of our fiber optic tweezers is where the particle is trapped, and rotated, that is, Fz = 0 pN as shown in Fig. 4(a). Working distance is the distance between working point and fiber end face. As in our initial conditions, the working distance is around 21 μm, which is very close to "pseudo focus" calculated before. Moreover, working distance is not sensitive to rotation angle.

Figure 4 shows the forces and torques exerted on the particle along the Z-axis with different rotation angles. Roughly speaking, trapping forces decrease, whereas in contrast, torques decrease as the rotation angle increases. This is because as the rotation angle increases, beams out of fiber cores become more divergent, which means tangent forces that rotate the particle become larger, whereas, the normal forces that trap become smaller. Therefore, there is an inevitable trade-off between trapping force and rotation torque, and we need to choose proper parameters in practice. We see that the rotation angle should be less than 8° when polished angle is 67° or the sphere will not be trapped anymore.

Figure 5 shows that the optimized rotation angle is around 4° that produces the greatest rotation angular speed, and the angular speed is relatively small compared with Black and Mohanty[5] because the sphere particle we modeled is most difficult to rotate due to its perfect symmetry, and to use circularly polarized input laser may improve the rotation frequency.

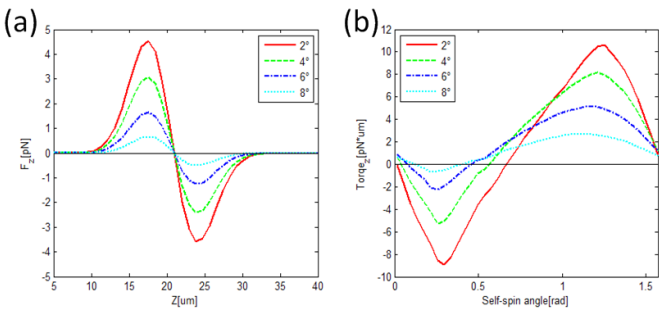

Fig. 4. Trapping forces along (a) the Z-axis and (b) torques with self-spin angle at working point at 67° polished angle with rotation angles 2°, 4°, 6°, and 8°.

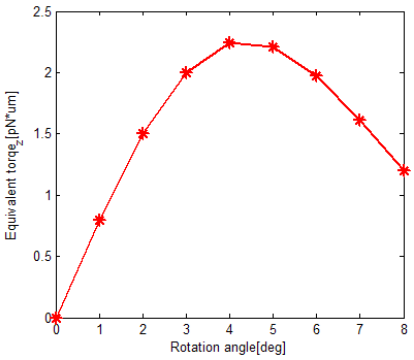

Fig. 5. Equivalent torques as a function of rotation angles from 0° to 9° with 67° polished angle.

Table 1. Rotation Torque Vectors versus Different Polishing Angle Errors

Group	**Four Polished Angles(°)**	**Most Unstable Rotation Torque Vector (pN*μm)**
0	67, 67, 67, 67	[0.00 0.00 4.02]
1	66.8, 67, 67, 67	[–0.44 0.00 4.21]
2	67.2, 67, 67, 67	[0.41 0.00 5.40]
3	66.8, 67.2, 67, 67	[–0.19 0.00 4.03]
4	66.8, 67.2, 67.2, 66.8	[–0.79 0.00 3.99]

It is worth noting that due to polishing errors, the polished angles cannot be exactly the same. The rotation axis of the trapped particle will not be parallel to the fiber axis (Z-axis) anymore. We have calculated out some discrete rotation torques according to different polished angles for each fiber core around 67° with 4° rotation angle as shown in Table 1. When the polished angle precision is controlled under ±0.2° (precision could be less restricted if the size of the particle becomes larger), the most unstable rotation torque minimum z component is much larger than maximum x and y components (almost five times even for the worst case). The rotation torque vector remain roughly the same, which means the rotation axis will change slightly due to polishing errors, but generally parallel to the fiber axis, which shows our method is a feasible approach.

In conclusion, we present a detailed numerical analysis of the trapping forces and rotation torque of a newly designed four-core fiber optic tweezers. By assessing the optical torque, the rotation function of polished angles is developed to evaluate the performance with a trapped micro-spheroid particle. Our study shows that there exists an optimized rotation angle so that the proposed fiber optic tweezers have the best performance.

This work was supported by the National Natural Science Foundations of China (Nos. 11274077 and 61290314), the 111 Project (No. B13015), and the Sino-Japan S & T cooperation project (Nos. 2010DFA-2770 and 2011DFB11520) at Harbin Engineering University.

References

1. A. Ashkin, J. Dziedzic, J. Bjorkholm, and S. Chu, Opt. Lett. **11,** 288 (1986).
2. D. G. Grier, Nature **424,** 810 (2003).
3. D. Van Thourhout and J. Roels, Nat. Photonics **4,** 211 (2010).
4. D. Baigl, Lab Chip **12,** 3637 (2012).
5. B. J. Black and S. K. Mohanty, Opt. Lett. **37,** 5030 (2012).
6. K. Taguchi, K. Atsuta, T. Nakata, and M. Ikeda, Opt. Commun. **176,** 43 (2000).
7. Y. Zhang, Z. Liu, J. Yang, and L. Yuan, J. Lightwave Technol. **30,** 1487 (2012).
8. A. Ashkin, Methods Cell Biol. **55,** 1 (1997).
9. A. M. Kowalevicz Jr and F. Bucholtz, "Beam divergence from an SMF-28 optical fiber," DTIC Document (2006).